Effect of packing parameter on phase diagram of amphiphiles: An off-lattice Gibbs ensemble approach

Geuorgui K. Bourov[a] and Aniket Bhattacharya[b]
Department of Physics, University of Central Florida, Orlando, Florida 32816-2385, USA

(Received 17 August 2007; accepted 17 October 2007; published online 28 December 2007)

We determine the phase diagram of several amphiphilic molecules as a function of the amphiphilic parameter α defined as the ratio of the volume of hydrophilic to hydrophobic segments using the Gibbs ensemble Monte Carlo method supplemented by configurational bias scheme. Specifically, we study amphiphilic molecules h_1t_7, h_2t_6, and h_3t_5, for which α=0.14, 0.33, and 0.60 respectively, and demonstrate that the former two exhibit phase separation while h_3t_5 forms micelles, supporting the contention that α=0.5 is the border line for phase separation and micellization, as observed in previous lattice Monte Carlo studies [Panagiotopoulos *et al.*, Langmuir **18**, 2940 (2002)]. Further, we study the phase separation in amphiphilic molecules as a function of the packing parameter by varying the size of the hydrophilic head for each molecule. We find that a larger hydrophilic head lowers the critical temperature T_c, and raises the critical density ρ_c. © *2007 American Institute of Physics*. [DOI: 10.1063/1.2807240]

I. INTRODUCTION

The determination of the phase diagram of complex molecules, e.g., polymers, amphiphiles, colloids, and their mixtures,[1–6] is necessary for the efficient use of these molecules in a wide variety of technological applications. Apart from their enormous usage in products of everyday life, the phase diagrams of these complex fluids exhibit special points or lines, and their confluence is of fundamental importance from a statistical mechanical perspective. Since the classic work of van der Waals for simple fluids, there has been a substantial amount of work directed towards the accurate characterization of phase diagram, critical exponents, and universality classes for systems with increasing levels of complexity. However, the determination of phase diagram, or the equation of state, is still most often hard to determine, excepting a few simple cases. The primary reason for such difficulty is that perturbative treatments fail in the vicinity of the critical points.

Computer simulation has played a major role in bridging the gap between theory and experiments in determining the critical properties of matter.[7,8] It is worth noting that in several cases development of new algorithms (e.g., Swendsen-Wang[9] to avoid the problem of critical slowing down) have effected significant breakthroughs, far more than what has been achieved by multiprocessor machines or faster chips. More recently the Wang-Landau[10] algorithm has been extended to study statistical mechanical properties of chain molecules. The Gibbs ensemble Monte Carlo (GEMC) technique due to Panagiotopoulos and Panagiotopoulos *et al.*[11–13] is another example of a significant advance in the algorithm development enabling the accurate determination of phase diagram for more complex molecules. The original development of GEMC technique has been further enriched by incorporating the configurational bias scheme by Smit and co-workers[14–16] into the GEMC method enhancing its efficiency for dense systems, specially for chain molecules. Soon after its inception and initial success with Lennard-Jones (LJ) molecules,[11,14] the GEMC method has been applied to chain molecules with significant degree of success.[17–22]

A few other theoretical and numerical developments have contributed significantly in determining the phase diagrams of complex molecules. On the theoretical side the thermodynamic perturbation theory by Wertheim[23–28] has been applied to chain molecules and has been compared with GEMC results. A parallel numerical approach known as the Gibbs-Duhem integration method has been claimed to be better suited for the determination of solid-liquid line and location of the triple point.[29,30] More recently, Charpentier and Jakse[31] have introduced an adaptive technique within the framework of integral equations to determine the phase diagram of complex fluids.

Amphiphilic molecules exhibit a rich and intriguing phase behavior and offer interesting fundamental problems as well as technical challenges in soft condensed matter physics. Each amphiphilic molecule contains a hydrophobic (tail) and a hydrophilic (head) segment linked by chemical bonds and spontaneously self-assemble[1–3] into a wide variety of structures depending upon the nature of the solvent, temperature, concentration, and packing consideration, e.g., the geometry and volume of the head and tail segments. Spherical and cylindrical micelles, bicontinuous and lamellar structures, vesicles, and other phases have been observed experimentally. Theoretical,[3,33,34] numerical mean field theory,[35,36] and computer simulation studies, using lattice[36–52] and continuum models,[53–63] have been able to reproduce some of the most important experimental results. Recent studies have

[a]Present address: Physical Science Department, Embry-Riddle Aeronautical University, Daytona Beach, FL 32114.
[b]Author to whom correspondence should be addressed. Electronic mail: aniket@physics.ucf.edu.

also been extended to look for conditions of complete phase separation, as opposed to micellization,[48,65,66] as a function of the ranges of attractive and repulsive interactions for the hydrophilic tail (t) and hydrophobic head (h) segments of the amphiphiles. Understanding self-assembling properties of amphiphilic molecules has recently become a very active field of research due to their widespread application in fabricating various devices and moieties at the nanometer length scales.[67,68]

Recently we have investigated how the effect of headgroup geometry affects the distribution, shape, and sizes of micelles by Brownian dynamics simulation.[63,64] In order to make the story complete, in this paper we apply GEMC method to study how the phase diagram of amphiphilic molecules is affected by the size of the hydrophilic head.

Although there have been several studies of lattice and off-lattice polymers using coarse grained models, they have not addressed the effect of head-group geometry adequately. In this work we demonstrate how the critical point and the first order line for an amphiphilic system shift as a function of the hydrophilic head size. We further demonstrate how the phase separation and micellization are affected by the continuous variation of the amphiphilic headgroup. The format of the rest of the paper is as follows. In the following section we describe the model and furnish specific details of the GEMC simulation. We present our results in Sec. III followed by summary and discussions in Sec. IV.

II. MODEL AMPHIPHILES AND SIMULATION METHODS

In our GEMC simulation an amphiphile is represented as $h_m t_n$ with m as hydrophilic head (h) beads and n as hydrophobic tail (t) beads connected by $m+n-1$ bonds. We use a bead-spring model for the amphiphiles so that the nonbonded potential acting between any two beads is chosen to be a LJ interaction and the interaction between two successive beads is given by a harmonic spring potential as given below.

$$U_{\mathrm{LJ}}^{ij}(r_{ij}) = 4\epsilon_{ij}\left[\left(\frac{\sigma_{ij}}{r_{ij}}\right)^{12} - \left(\frac{\sigma_{ij}}{r_{ij}}\right)^{6} - \left(\frac{\sigma_{ij}}{r_{ij}^{c}}\right)^{12} + \left(\frac{\sigma_{ij}}{r_{ij}^{c}}\right)^{6}\right]; \quad r \leqslant r_{ij}^{c}, \tag{1a}$$

$$U_{\mathrm{bond}}(r_{ij}) = \frac{V_{\mathrm{spring}}}{2}(r_{ij} - r_0)^2, \tag{1b}$$

where r_{ij}^{c} is the cutoff distance beyond which the LJ interaction is set to be zero, $r_{ij}=|\vec{r}_i-\vec{r}_j|$, and $\vec{r}_i$ and $\vec{r}_j$ are the locations of the ith monomers, respectively. *Amphiphilicity* in this model is introduced by a repulsive cutoff distance for the head-head and head-tail ($r_{hh}^{c}=2^{1/6}\sigma_{hh}$ and $r_{ht}^{c}=2^{1/6}\sigma_{ht}$) interactions, and an attractive tail-tail interaction with the cut-off distance being always equal to the half the instantaneous length of the simulation box. V_{spring} and r_0 are the energy and the length parameters of the harmonic potential, respectively. We have chosen $V_{\mathrm{spring}}=2000$ and $r_0=1.0$. Simulations of the Gibbs ensemble are performed in two separate simulation boxes, each having periodic boundary conditions. The initial configurations of molecules are created randomly and then the system is equilibrated for 2.0×10^5 GEMC cycles.

To achieve phase coexistence during the simulation four conditions need to be satisfied. The temperature T, pressure P, and chemical potential μ need to be kept the same in both boxes; additionally, each subsystem has to remain in thermodynamic equilibrium. Since the temperature T is an input parameter in the simulation, the remaining three conditions are satisfied by performing three types of *move*: (i) displacement of molecules into each subsystem, (ii) correlated fluctuation of the subsystem's volumes, and (iii) transfer of molecules between the boxes. In the following paragraph we discuss some details of the simulation.

In the *displacement move*, a randomly selected bead has a chance to be displaced of a random length along a random direction. The maximum value of the displacement in the entire simulation is set to $\Delta r=0.1\sigma_{tt}$. In addition to the displacement of a single bead in an amphiphile, the center of mass of the molecule is also randomly displaced. In our simulations, there are no explicit solvent molecules and the effect of the solvent is incorporated through the bead-bead interactions.

The *volume change* of the boxes, as mentioned before, is done in such a way that the total volume accessible to the system is constant. We change each simulation compartment by a random rescaling of the volume of one of the two compartments V_1 or V_2 with the constraint that the total volume $V=V_1+V_2$ is preserved. Without lost of generality, we use cubic boxes. Initially they have the same volume, but with the evolution of the system the two boxes are adjusted so that the densities of the two phases trace the coexistence curve. The maximum volume change is set to $\Delta V/V=0.1$ and the positions of the amphiphiles are recalculated by rescaling the center of the mass of each amphiphile. The attractive cut-off distance is also adjusted to the half the length of the simulation box every time a volume change move is accepted.

For the *exchange move*, a molecule is selected randomly from either of the boxes as a candidate for replacement to the other box. The initial configurational energy of the molecule $U(old)$ and the Rosenbluth factor $W_{\mathrm{old}}^{\mathrm{ext}}$ are calculated. Starting from an arbitrary position the whole molecule is regrown by the configurational-bias method. The configurational energy $U(new)$ of the regrown molecule is calculated and the decision of acceptance is made by the rules for GEMC method.[8] Additionally, the number of exchange moves are restricted in the range of 1%–5% so that the system has enough time to equilibrate. The whole process of the insertion of an amphiphile molecule is governed by the decreases of the free energy. The configurational energies calculated in simulation can be used to obtain the chemical potential.

Changing the box sizes and the number of molecules in each box leads to different densities in the boxes. Therefore, the phase coexistence densities are obtained in a single simulation without having prior knowledge of the phase properties of the system. It is worth mentioning that the choice of the initial densities affects the computational time needed to equilibrate the system. If the initial conditions are chosen in such way that the densities are in an unstable region[32] where $\partial P/\partial V>0$, the evolution of the system goes in the direction of stable phases and pressures. However, if initially the system is in a metastable region, then the system is thermody-

namically stable and we cannot expect a phase separation unless a huge fluctuation removes the system from this metastable state. In the case of a known phase diagram, the initial densities can be chosen to be close to the ones expected. Since the aim of our simulations is to obtain unknown phase diagrams we perform several probing runs and the appropriate initial densities are chosen. We have checked that the resulting phase diagram does not depend on the initial density conditions but equilibration and collection of statistical averages are greatly affected by the input densities and number of molecules in each region.

Close to the critical temperature T_c, Gibbs ensemble simulations cannot provide information for the coexisting phases. The method we have used for the estimation of the critical point is to fit the obtained phase coexistence points according to the law of rectilinear diameters.[70] This law relates the densities of the liquid phase ρ_l, gas phase ρ_g, and critical density ρ_c to the critical temperature T_c,

$$\frac{\rho_l + \rho_g}{2} = \rho_c + A(T - T_c). \tag{2}$$

III. RESULTS

We first study the phase diagram of homopolymers of length 2 (t_2) and 8 (t_8), previously investigated by others,[20–22] to check the accuracy and validity of the simulation code that we developed.[71] These are presented in Secs. III A and III B, respectively. In Sec. III C we present detailed results for the phase diagram of amphiphiles.

A. Phase diagram of t_2

The phase diagram of dimers with a fixed bond length was obtained by Vega *et al.*[22] The model of a dimer of fixed bond length can be considered as the limiting case of the bead-spring model when the spring constant $k \to \infty$. We have studied a system consisting of 400 bead-spring dimers initially divided equally between the two compartments. We have performed 10^5 GEMC cycles and collected data for 10^4 states of the system. In each GEMC cycle we perform all the three types of moves in a random sequence as described in the previous section. Vega *et al.* carried out 2×10^4 cycles of constant-volume *N-V-T* Monte Carlo in such a system and used the final configuration of the *N-V-T* MC runs as the starting point of their GEMC calculations. They used initial vapor and liquid densities close to the expected coexistence values.

We start out with a completely different initial condition. We begin simulations with the same density of amphiphiles in both boxes. In particular, we have chosen an initial molecular density of each box to be $\rho_{\mathrm{mol}}=0.15$, which corresponds to a monomer (bead) density of $\rho=0.3$. The length L of the cubic simulation box is calculated from the density ρ_{mol} as $L=(N/2\rho_{\mathrm{mol}})^{1/3}$. For the purpose of testing of the code, we have used configurational bias to grow the chains, although not necessary for dimers,

The computed phase diagram is shown in Fig. 1, together with the phase coexistence points obtained by Vega *et al.*[22] We notice that the fixed bond length GEMC results of

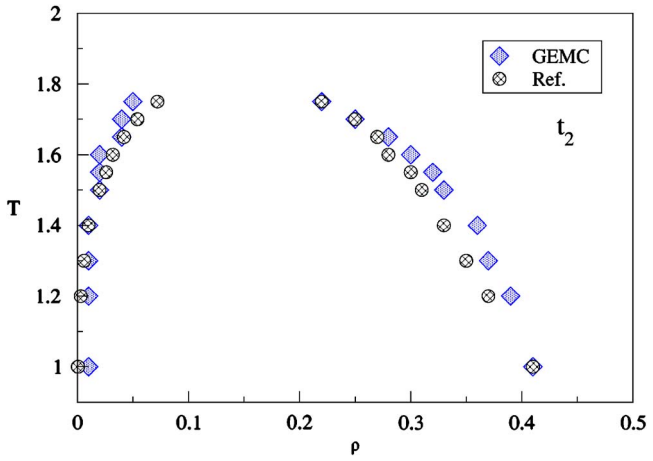

FIG. 1. (Color online) Phase diagram for dimers (t_2). The hatched (blue online) diamonds are from GEMC simulations and the circles with crosses are from Vega *et al.* (Ref. 22).

Vega *et al.* (without using configurational bias) are in close agreement with ours. Our results at a temperature $T=1.6$ produce a slightly higher packing density due to bond-length fluctuations of 5%–8%.

B. Phase diagrams of t_8

We have next determined the phase diagram of a bead-spring polymer chain of length 8 (t_8) by the same method used for dimers. Our results are shown in Fig. 2 together with the coexistence points calculated in Ref. 20. The critical temperature for t_8 is estimated to be $T_c=2.69$. The bead-spring model of homopolymers can be considered as model for alkanes. It is well known that below the critical temperature alkanes exhibit a first-order phase transition between a low-density gas and high-density liquid phases. These two phase diagrams for t_2 and t_8 are shown in Figs. 1 and 2, respectively, and extracted using our GEMC simulation code which captures the essential features of phase separation and the presence of a critical temperature T_c. We now use the same method to study phase separation and micellization of amphiphilic molecules.

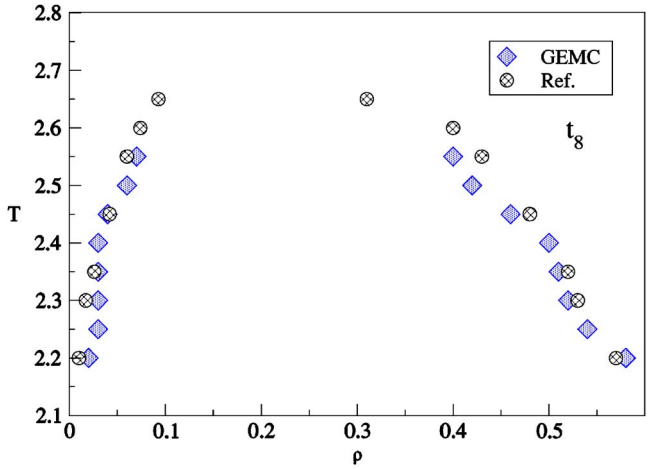

FIG. 2. (Color online) Phase diagram for t_8. The hatched (blue online) diamonds are from GEMC simulations and the circles with crosses are from Escobedo *et al.* (Ref. 20).

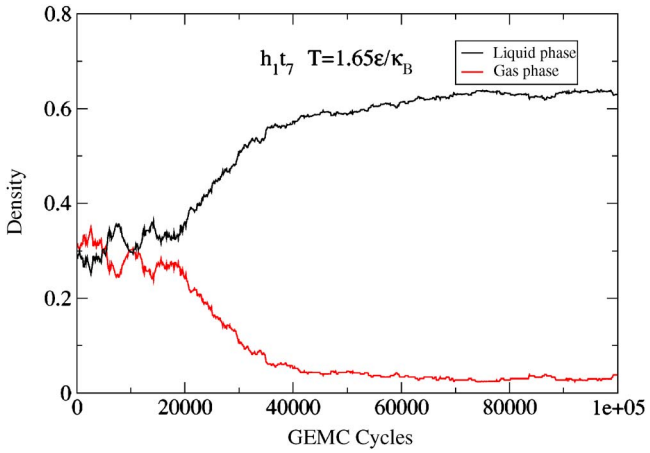

FIG. 3. (Color online) Density evolution in two subsystems of h_1t_7 during GEMC simulation at a reduced temperature $T=1.65$.

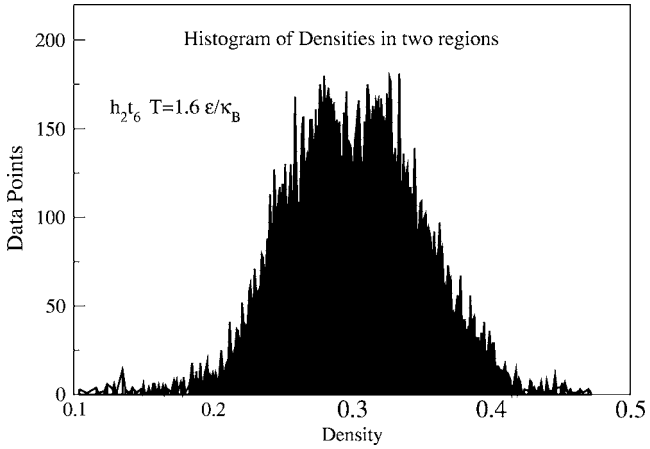

FIG. 5. The histogram of evolution of densities during GEMC simulation for h_2t_6 corresponding to Fig. 5.

C. Phase diagrams of amphiphiles: Micellization vs phase separation

Here we present GEMC simulation results for amphiphilic molecules. In order to determine how the amphiphilicity (ratio of hydrophilic to hydrophobic units) affects the phase separation, we continue to study the chains of length 8. This section is divided into two parts. We first study amphiphiles constructed of identical beads. In the next subsection we vary the size of the hydrophilic head.

1. Amphiphiles with building blocks of same size

We have investigated the phase diagram for h_1t_7, h_2t_6, and h_3t_5. These model amphiphiles bear close similarity with the poly(oxyethylene) surfactants as follows:

$$h_1t_7 \rightarrow C_{21}E,$$

$$h_2t_6 \rightarrow C_{18}E_2, \tag{3}$$

$$h_3t_5 \rightarrow C_{15}E_3.$$

To give an idea how one obtains points of the first order line in the density-temperature plane we show here some actual data for the evolution of densities in two boxes as a function of the GEMC simulation steps. For our first example, we show in Fig. 3 the density evolution for h_1t_7. Next, keeping the length of the chain the same, we change the length of the hydrophilic and the hydrophobic segments from 1 and 7 (h_1t_7) to 2 and 6 (h_2t_6), respectively. The corresponding density variations for h_2t_6 are shown in Fig. 4. When we compare Fig. 4 with Fig. 3, we notice that for h_2t_6 the relative difference in respective densities is small compared to the case for h_1t_7. This implies that the simulation temperature is close to the critical temperature of the system leading to a large fluctuation of the densities as shown in Fig. 4, and the GEMC method cannot give correct predictions. In this case, a plot of the histogram of the densities is more useful as shown in Fig. 5, where the two peaks corresponding to the densities of two separate phases close to the critical density still could be identified. The phase diagrams of h_1t_7 and h_2t_6 are given on Fig. 6. The estimated critical temperatures for h_1t_7 and h_2t_6 from the plots are 1.97 and 1.6, respectively. We notice that increasing the ratio of the hydrophilic to hydrophobic part of the molecules from 1:7 to 2:6 results in decreasing the critical temperature of the system.

It is worth mentioning that Panagiotopoulos *et al.* have studied the problem of phase separation versus micellization using grand canonical Monte Carlo simulations[69] of diblock

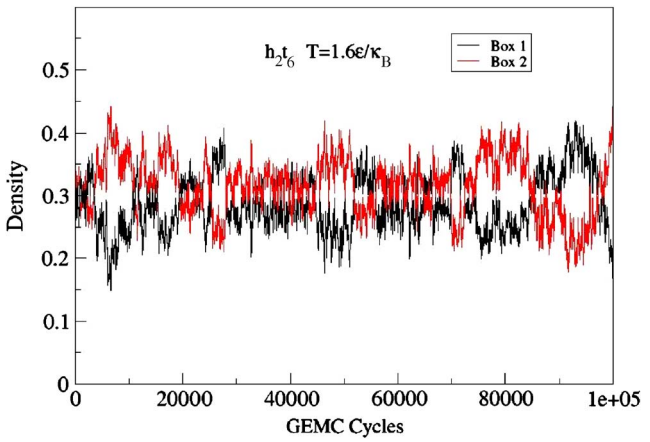

FIG. 4. (Color online) Density evolution in two subsystems of h_2t_6 during GEMC simulation at a reduced temperature $T=1.6$.

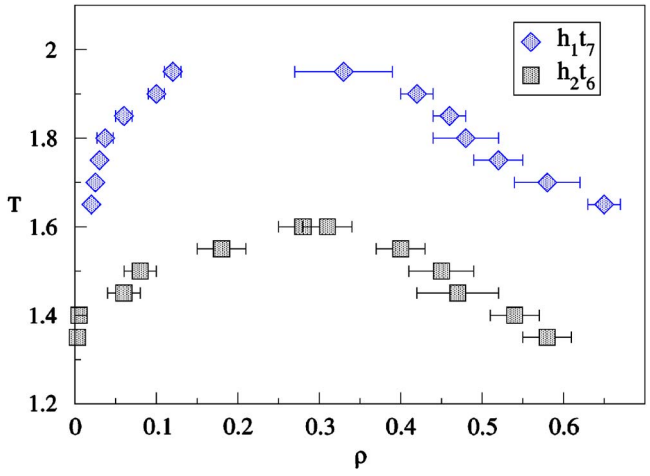

FIG. 6. (Color online) Comparison of the phase diagrams for h_1t_7 and h_2t_6.

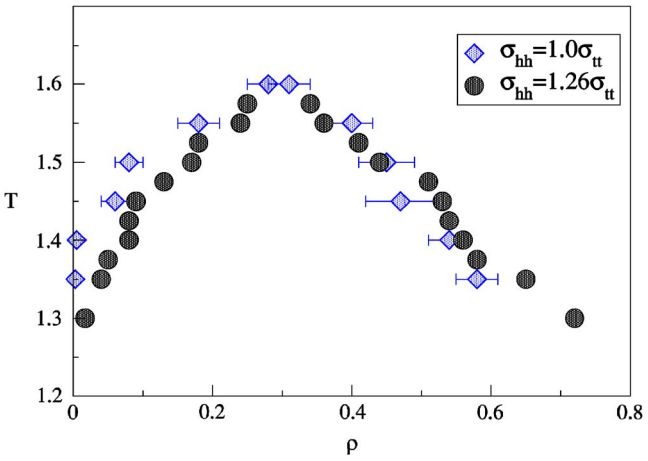

FIG. 7. (Color online) A comparison of phase diagrams for h_2t_6 (blue hatched diamonds) and $h_1^{1.26}t_6$ (circles).

and triblock surfactants. They conclude that a specific amphiphile h_xt_y can display either micellization or a macroscopic phase separation but not both. From our off-lattice GEMC results we conclude that increasing the hydrophilic part of an amphiphile leads to a less tendency for phase separation and hence favors micellization.

2. Amphiphiles with large head group

In this section we present results that show how the phase diagram is affected by the head group geometry. Our goal is to calculate the phase diagram for h_1t_6 with a larger hydrophilic bead of size $\sigma_{hh}=1.26\sigma_{tt}$. Let us denote it as $h_1^{1.26}t_7$. The choice is guided by the fact that $h_1^{1.26}t_6$ has the same hydrophilic and hydrophobic volumes as that of h_2t_6 (volume is calculated using LJ diameters). Phase diagrams for both of these molecule are shown in Fig. 7. We notice that both systems show phase separation. However it is evident that compared to the first order line for h_2t_6, the corresponding line for $h_1^{1.26}t_7$ is shifted to a lower temperature. This will become more conclusive by later in Fig. 11.

In addition to h_1t_7 and h_2t_6 we also studied h_3t_5. After exploring a wide range of temperatures, we find that this system does not phase separate. When we look at the cluster distribution[72] for h_3t_5, shown in Fig. 8, we notice the presence of several large aggregates with average sizes from 130 to 148 amphiphiles, as well as several small aggregates with sizes less than 5.

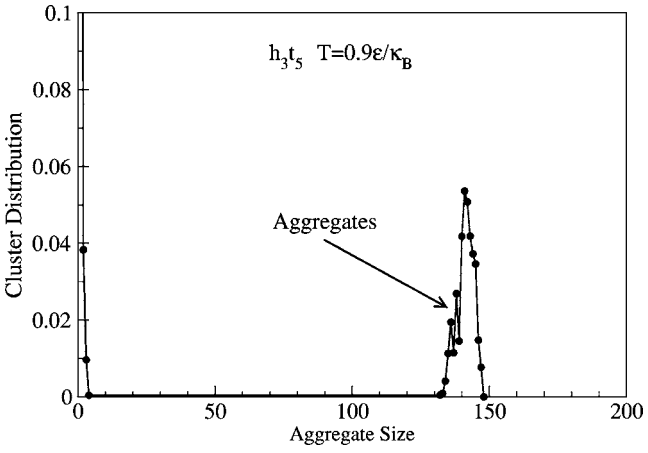

FIG. 8. Cluster distribution for h_3t_5 amphiphiles.

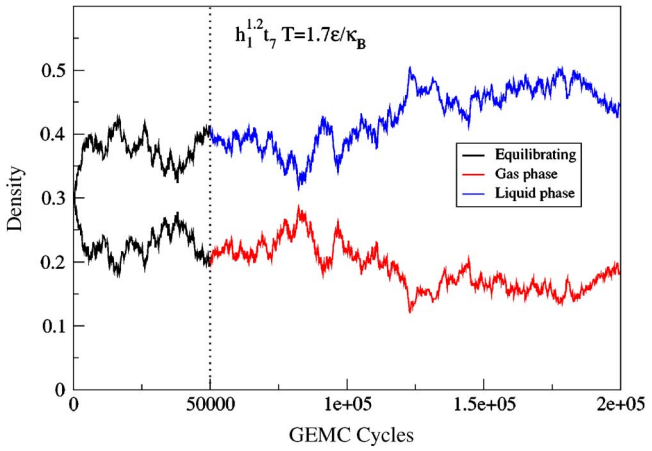

FIG. 9. (Color online) GEMC evolution of the density of the liquid and gas phases at $T=1.75$ for $h_1^{1.2}t_7$. First 50 000 GEMC cycles are used to equilibrate the system.

We complete this set of studies by investigating the phase diagram of amphiphiles for a fixed tail length as a function of the volume of a single hydrophilic head. In other words we study the phase diagram as a function of the packing parameter.[3] In particular, we simulate amphiphiles with head sizes of $\sigma_{hh}=\sigma_{tt}$, $\sigma_{hh}=1.1\sigma_{tt}$, and $\sigma_{hh}=1.2\sigma_{tt}$. These we, respectively, denote as h_1t_7, $h_1^{1.1}t_7$, and $h_1^{1.2}t_7$. Starting with an initial density 0.3 in both the simulation boxes, the subsequent evolution of densities for $h_1^{1.2}t_7$ are shown in Figs. 9 and 10 for temperatures $T=1.75$ and $T=1.80$, respectively. Close to the critical temperature (Fig. 10), fluctuations in the boxes increases and we use the histogram of the respective densities, as shown earlier, to calculate average density in each box. The phase diagrams of three systems with different hydrophilic head sizes are shown in Fig. 11. T_c is extrapolated from a straight line fit to these points for each case using Eq. (2). From the simulation data, we conclude that with the increasing hydrophilic head size (which effec-

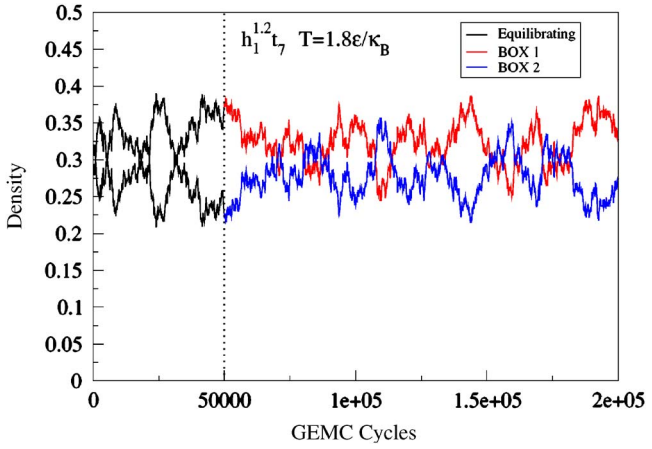

FIG. 10. (Color online) GEMC evolution of the density of the liquid and gas phases at $T=1.8$ for $h_1^{1.2}t_7$. First 50 000 GEMC cycles are used to equilibrate the system.

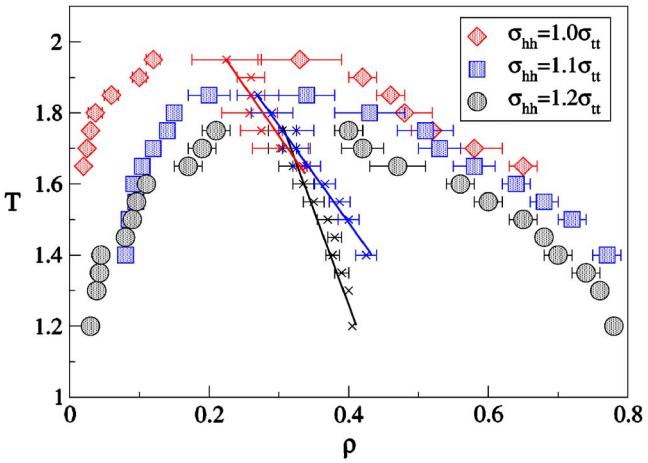

FIG. 11. (Color online) Phase diagrams for h_1t_7, $h_1^{1.1}t_7$, and $h_1^{1.2}t_7$. The straight lines are extracted using Eq. (2).

tively lowers the packing parameter) the critical temperature T_c of the amphiphilic system decreases while the critical density ρ_c increases.

IV. CONCLUSION

In this work, we have studied phase separation and micellization of model amphiphilic molecules represented as hydrophobic and hydrophilic beads connected by anharmonic springs using an off-lattice GEMC simulation method. Specifically we studied how the hydrophilic head of different sizes affect the phase separation process. We have tested the code by studying similar systems previously investigated by others. For example, we have studied bead-spring homopolymers of chain lengths 2 and 8 and compared the phase diagrams with those obtained previously for fixed bond models of alkanes. We have also deliberately chosen different initial conditions to check the convergence of the GEMC method.

We then addressed the issue of phase separation versus micellization in an amphiphilic system as demonstrated earlier in the lattice GCMC simulation. Specifically we considered three amphiphilic molecules h_1t_7, h_2t_6, and h_3t_5, respectively, and used GEMC method to determine the phase diagram of these molecules. The amphiphilicity α defined in terms of ratio of the hydrophilic to hydrophobic segments for these molecules are, respectively, 0.14, 0.33, and 0.6. While for h_1t_7 and h_2t_6 we have been able to obtain the first order line and hence the critical temperature and density, we found that h_3t_5 (for which α=0.6) does not exhibit phase separation, rather, as we found from the cluster distributions, they form micelles. These studies are independent verification of the contention that α=0.5 is the borderline for phase separation and micellization.

Since our simulations are carried out in continuum, for a given tail length we can vary the size of the hydrophilic head and hence change the packing parameter continuously. Thus, we have been able to determine the phase diagrams of amphiphiles as a function of the packing parameter of the individual molecules and study how the packing parameter affects the critical point in the ρ-T plane. We observe in a systematic fashion that the critical temperature is reduced and the critical density is increased as the hydrophilic segment of the molecule is enlarged. In addition, from Fig. 11 we note that starting with a system having the smallest hydrophilic head group as a reference, as one increases the hydrophilic head segment, there is a systematic shift of the first order line towards lower temperature. These studies are our first steps towards determining the phase diagram of more complex molecules of arbitrary shape in the near future using configurational biased GEMC method.

ACKNOWLEDGMENTS

The research reported here is supported in part from the National Science Foundation NIRT (ENG/ECS and CISE/EIA) under Grant No. 0103587. We thank Weili Luo and Kevin Belfield for numerous discussions.

[1] R. G. Larson, *The Structure and Rheology of Complex Fluids* (Oxford University Press, New York, 1999).
[2] S. A. Safran, *Statistical Thermodynamics of Surfaces, Interfaces, and Membranes* (Addison Wesley, New York, 1994).
[3] J. N. Israelachvili, *Intermolecular and Surface Forces* (Academic, New York, 1985).
[4] K. Holmberg, B. Jönsson, B. Kronberg, and B. Lindman, *Surfactants and Polymers in Aqueous Solution* (Wiley, New York, 2003).
[5] S. Karaborni and B. Smit, Curr. Opin. Colloid Interface Sci. **1**, 411 (1996).
[6] W. M. Gelbart and A. Ben-Shaul, *Micelles, Membranes, Microemulsions and Monolayers* (Springer-Verlag, New York, 1994).
[7] M. P. Allen and D. J. Tildesley *Computer Simulation of Liquids* (Clarendon, Oxford, 1989).
[8] D. Frenkel and B. Smit, *Understanding Molecular Simulations* (Academic, New York, 2002).
[9] R. H. Swendsen and J.-S. Wang, Phys. Rev. Lett. **58**, 86 (1987).
[10] F. Wang and D. P. Landau, Phys. Rev. Lett. **86**, 2050 (2001).
[11] A. Z. Panagiotopoulos, Mol. Phys. **61**, 813 (1987).
[12] A. Z. Panagiotopoulos, N. Quirke, M. Stapleton, and D. J. Tildesley, Mol. Phys. **63**, 527 (1988).
[13] For a review see A. Z. Panagiotopoulos, J. Phys.: Condens. Matter **12**, R25 (2000).
[14] B. Smit, Ph. de Smedt, and D. Frenkel, Mol. Phys. **68**, 931 (1989).
[15] B. Smit and D. Frenkel, Mol. Phys. **68**, 951 (1989).
[16] J. L. Siepmann and D. Frenkel, Mol. Phys. **75**, 59 (1992).
[17] G. C. A. M. Mooij, D. Frenkel, and B. Smit, J. Phys.: Condens. Matter **4**, L255 (1992).
[18] M. Laso, J. J. de Pablo, and U. W. Sutter, J. Chem. Phys. **97**, 2817 (1992).
[19] B. Smit, S. Karaborni, and I. Siepmann, J. Chem. Phys. **102**, 2126 (1995).
[20] F. A. Escobedo and J. J. de Pablo, Mol. Phys. **87**, 347 (1996).
[21] F. J. Blasand L. F. Vega, Mol. Phys. **92**, 1 (1997).
[22] C. Vega, C. McBride, E. de Miguel, F. J. Blas, and A. Galindo, J. Chem. Phys. **118**, 10696 (2003).
[23] M. S. Wertheim, J. Stat. Phys. **35**, 19 (1984); **35**, 35 (1984); **42**, 459 (1986); **42**, 477 (1986).
[24] G. Jackson, W. G. Chapman, and K. E. Gubbins, Mol. Phys. **65**, 1 (1988).
[25] M. S. Wertheim, J. Chem. Phys. **87**, 7323 (1987).
[26] W. G. Chapman, G. Jackson, and K. E. Gubbins, Mol. Phys. **65**, 1057 (1988).
[27] J. K. Johnson, J. A. Zollweg, and K. E. Gubbins, Mol. Phys. **78**, 591 (1993).
[28] J. K. Johnson, E. A. Müller, and K. E. Gubbins, J. Phys. Chem. **98**, 6413 (1994).
[29] D. A. Kofke, Mol. Phys. **78**, 1331 (1993).
[30] D. A. Kofke, J. Chem. Phys. **98**, 4149 (1993).
[31] I. Charpentier and N. Jakse, J. Chem. Phys. **123**, 204910 (2005).
[32] For a review, see J. D. Gunton, M. San Miguel, and P. S. Sahni, in *Phase Transition and Critical Phenomena*, edited by C. Domb and J. L. Lebowitz (Academic, London, 1983), Vol. 8.

[33] D. Blankschtein, G. M. Thurston, and G. B. Benedek, Phys. Rev. Lett. **54**, 955 (1985); G. M. Thurston, D. Blankschtein, M. R. Fisch, and G. B. Benedek, J. Chem. Phys. **84**, 4558 (1986); D. Blankschtein, G. M. Thurston, and G. B. Benedek, *ibid.* **85**, 7268 (1986); S. Puvvada and D. Blankschtein, *ibid.* **92**, 3710 (1990).
[34] A. Ben-Shaul, I. Szleifer, and W. M. Gelbart, J. Chem. Phys. **83**, 3597 (1985); I. Szleifer, A. Ben-Shaul, and W. M. Gelbart, *ibid.* **83**, 3612 (1985).
[35] C. M. Wijmans and P. Linse, Langmuir **11**, 3748 (1995).
[36] A. D. Mackie, A. Z. Panagiotopoulos, and I. Szleifer, Langmuir **13**, 5022 (1997).
[37] R. G. Larson, L. E. Scriven, and H. T. Davis, J. Chem. Phys. **83**, 2411 (1985); R. G. Larson, *ibid.* **89**, 1642 (1988); **91**, 2479 (1989); J. Chem. Phys. **96**, 7904 (1992); J. Phys. II **6**, 1441 (1996).
[38] C. M. Care, J. Phys. C **20**, 689 (1987).
[39] C. M. Care, J. Chem. Soc., Faraday Trans. **83**, 2905 (1987).
[40] D. Brindle and C. M. Care, J. Chem. Soc., Faraday Trans. **88**, 2163 (1994).
[41] J.-C. Desplat and C. M. Care, Mol. Phys. **87**, 441 (1996).
[42] A. T. Bernardes, V. B. Henriques, and P. M. Bisch, J. Chem. Phys. **101**, 645 (1994).
[43] A. T. Bernardes, J. Phys. II **6**, 169 (1996).
[44] P. H. Nelson, G. C. Rutledge, and T. A. Hatton, J. Chem. Phys. **107**, 10777 (1997).
[45] Aniket Bhattacharya and S. D. Mahanti, J. Phys.: Condens. Matter **12**, 6141 (2000).
[46] Aniket Bhattacharya and S. D. Mahanti, J. Phys.: Condens. Matter **13**, L861 (2001).
[47] A. Floriano, E. Caponetti, and A. Z. Panagiotopoulos, Langmuir **15**, 3143 (1999).
[48] S. Salaniwal, S. K. Kumar, and A. Z. Panagiotopoulos, Langmuir **19**, 5164 (2003).
[49] C. S. Shida and V. B. Henriques, J. Chem. Phys. **115**, 8655 (2001).
[50] A. Milchev, A. Bhattacharya, and K. Binder, Macromolecules **6**, 1881 (2001).
[51] D. Viduna, A. Milchev, and K. Binder, Macromol. Theory Simul. **7**, 649 (1998).
[52] L. A. Rodriguez-Guadarrama, S. K. Talsania, K. K. Mohanty, and R. Rajagopalan, Langmuir **15**, 437 (1999).
[53] D. R. Rector, F. van Swol, and J. R. Henderson, Mol. Phys. **82**, 1009 (1994).
[54] B. Smit, K. Esselink, P. A. Hilbert, N. M. van Os, L. A. M. Rupert, and I. Szleifer, Langmuir **9**, 9 (1993); B. Smit, P. A. Hilbert, K. Esselink, L. A. M. Rupert, and N. M. van Os, J. Chem. Phys. **95**, 6361 (1991).
[55] B. Palmer and J. Liu, Langmuir **12**, 746 (1996); , J. Chem. Phys. **12**, 6015 (1996).
[56] F. K. von Gottberg, K. A. Smith, and T. A. Hatton, J. Chem. Phys. **106**, 9850 (1997).
[57] R. Goetz and R. Lipowsky, J. Chem. Phys. **108**, 7397 (1998).
[58] A. Bhattacharya, A. Chakrabarti, and S. D. Mahanti, J. Chem. Phys. **108**, 10281 (1998).
[59] J.-B. Maillet, V. Lachet, P. V. Coveney, Phys. Chem. Chem. Phys. **1**, 5277 (1999).
[60] T. Soddemann, B. Dunweg, and K. Kremer, Eur. Phys. J. E **409**, 409 (2001).
[61] S. Bogusz, R. M. Venable, and R. Pastor, J. Phys. Chem. **105**, 8312 (2001).
[62] P. K. Maiti, Y. Lansac, M. A. Glaser, N. A. Clark, and Y. Roualt, Langmuir **18**, 1908 (2002).
[63] G. Bourov and A. Bhattacharya, J. Chem. Phys. **119**, 9219 (2003); **122**, 044702 (2005).
[64] G. Bourov and A. Bhattacharya, J. Chem. Phys. **123**, 204712 (2005).
[65] V. Kapila, J. M. Harris, P. A. Deymer, and S. Raghavan, Langmuir **18**, 3728 (2002).
[66] B. Owenson and L. R. Pratt, J. Phys. Chem. **88**, 2905 (1984).
[67] Z. Zhang, M. A. Horsch, M. Lamm, and S. C. Glotzer, Nano Lett. **3**, 1341 (2003).
[68] C. Sangregorio, J. K. Wiemann, C. J. O'Connor, and Z. Rosenzweig, J. Appl. Phys. **85**, 5699 (1999).
[69] A. Z. Panagiotopoulos, M. A. Floriano, and S. K. Kumar, Langmuir **18**, 2940 (2002).
[70] J. S. Rawlinson and F. L. Swinton, *Liquids and Liquid Mixtures* (Butterworths, London, 1982).
[71] G. Bourov, Ph.D. dissertation, University of Central Florida, 2005.
[72] We define two molecules belong to the same cluster if the distance between any two hydrophobic beads from molecules is less than $2.5\sigma_{tt}$.